

Characteristics of SAR Images of Man-Made Objects – A Comparison with Respect to Aspect Angle and Frequency

Patrick Berens, Michael Caris, and Ingo Walterscheid

Fraunhofer FHR – GERMANY

patrick.berens@fhr.fraunhofer.de

ABSTRACT

During a measurement campaign of the NATO research group SET-250 SAR measurements have been performed with two SAR sensors of Fraunhofer FHR using different frequency bands: the MIRANDA-94 and the PAMIR-Ka. We processed the data to create SAR images with approximately 10 cm resolution in both range and cross range direction and analysed the results. The main objective of the joint measurement campaign was to collect multi-dimensional radar data of military objects, where the designation ‘multi-dimensional’ covered various parameters, e.g., illumination direction, frequency, polarisation, and time. Beyond the mentioned SAR imaging the data of each sensor was used with respect to specific additional capabilities. While MIRANDA-94 was used to evaluate the benefit of polarimetric measurements, we varied PAMIR-Ka processing parameters to evaluate the advantages of multiple looks with respect to frequency and illumination direction.

1.0 INTRODUCTION

In summer 2019, Fraunhofer FHR participated with two SAR sensors in a joint measurement campaign organized by the NATO SET-250 research task group. The motivation of the mission was to collect radar data of military targets with a broad range of different parameters, to analyse the results of the acquisitions against each other, and last but not least to combine them to increase the overall knowledge about the targets. The gain of information gives additional potential for a subsequent Automatic Target Recognition (ATR) process, which however lies outside the scope of the SET-250. This motivates a close cooperation with the SET-273, which among other matters deals with ATR.

Ref. [1] gives a good overview about the participating sensors and the measurements of the joint campaign. We here concentrate on the measurements of the two sensors from Fraunhofer FHR, the PAMIR-Ka with a centre frequency of 35 GHz and the W-band system MIRANDA-94. An ultra-light aircraft carried both sensors alternately during the campaign. While PAMIR-Ka is a pulse radar, MIRANDA-94 applies the FMCW principle. Detailed descriptions of the hardware of the systems are given in Refs. [2], [3], and [4].

The following sections contain different aspects of the data analyses of the two radar systems. Section 2.0 focusses on multi-aspect SAR imaging. Here we present SAR images of some military targets illuminated from different directions using the Ka- and the W-band. In Section 3.0, we focus on the polarimetric feature of MIRANDA-94: Vertical and horizontal components of the backscattered echoes are received by two independent channels. After that, Section 4.0 addresses multi-look processing, which is possible for PAMIR-Ka because the acquired data have a wide illumination angle and a bandwidth much higher than needed for the 10 cm high resolution. We use multiple looks in two different kinds: On one hand, we perform incoherent combination to get a better image (contrast enhancement, speckle reduction) and on the other hand, we analyse the appearance of a special man-made object in different single looks. Finally, Section 5.0 gives a conclusion.

2.0 MULTI-ASPECT SAR IMAGING IN KA- AND W-BAND

The joint contribution [1] of the participants of the NATO SET-250 measurement campaign in England describes the flight geometries of the ultra-light aircraft during the SAR acquisitions of PAMIR-Ka and MIRANDA-94. Both systems illuminated the scene from eight different directions so that complementary information was gathered. Figure 1 shows the central part of a scene with three military targets at positions A, B, and C. Targets A and C are mobile surface-to-air missile systems equipped with three missile mock-ups. Target B is also a tracked vehicle, which is equipped with a radar station.



Figure 1: Google Earth image of the scene in England with three marked targets

We processed the data and compared the resulting SAR images of our two radar systems. We selected four of the eight illumination directions and exclude the remaining directions from the following discussions. Figure 2 shows the SAR images of target A. The left column shows the SAR images acquired in the Ka-band using the PAMIR system and the right column contains the W-band results of the MIRANDA. Note that the radar acquisition could not be done at the same time because the ultra-light aircraft was not able to carry both systems simultaneously. The illumination directions of the four rows belong to the planned cardinal illumination directions 158° , 248° , 338° , and 23° , respectively. The illumination directions can be assigned according to the shadowing. As PAMIR-Ka did not compensate for aircraft drift, which was large during the acquisitions, the true illumination directions of PAMIR-Ka differ from the planned values by small angles. They amount to 155° , 243° , 344° , and 30° . For comparisons of the SAR images, it is important to note that they are given in local ENU (East, North, Up) coordinates.

In the first row, target A is illuminated from the side. In this orientation, the length of the target can be evaluated from the SAR images. For both SAR systems, the shadows of three missiles can be identified. The illumination in the second row is approximately in longitudinal direction. The resulting SAR images let us determine the width of the target. The third row contains the other side view of the target. The PAMIR image shows up six parallel structures that occur from the three missiles. The MIRANDA image also contains reflections from the missiles. However, they do not have a comparably regular structure.

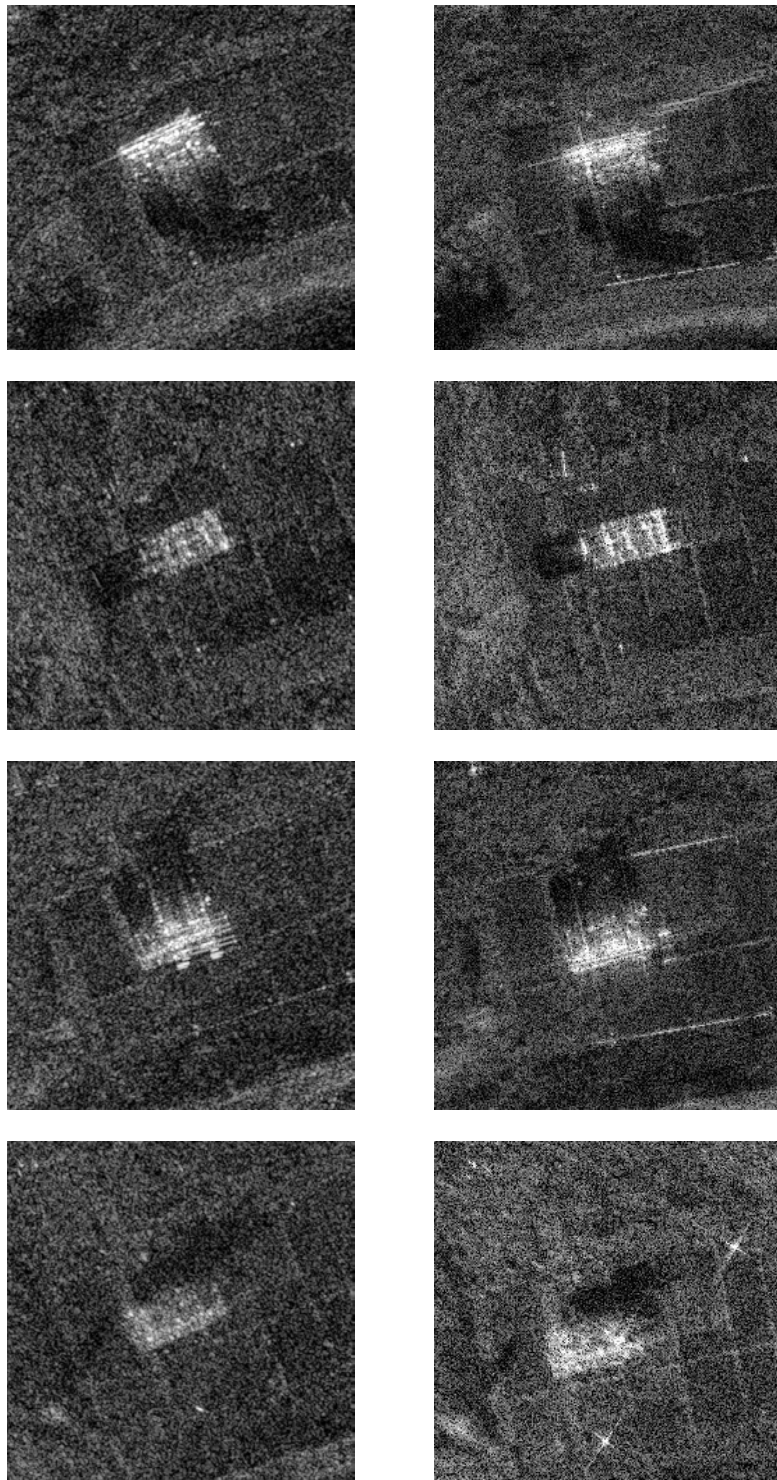


Figure 2: Images of target A; left and right column show PAMIR-Ka and MIRANDA-94 results, respectively

The images of PAMIR-Ka and MIRANDA-94 seem to be quite similar. However, due to the shorter wavelength of the MIRANDA system, the SAR images of this system feature more reflections from small-scale structures. This can be seen especially with respect to the structure of the ground clutter.

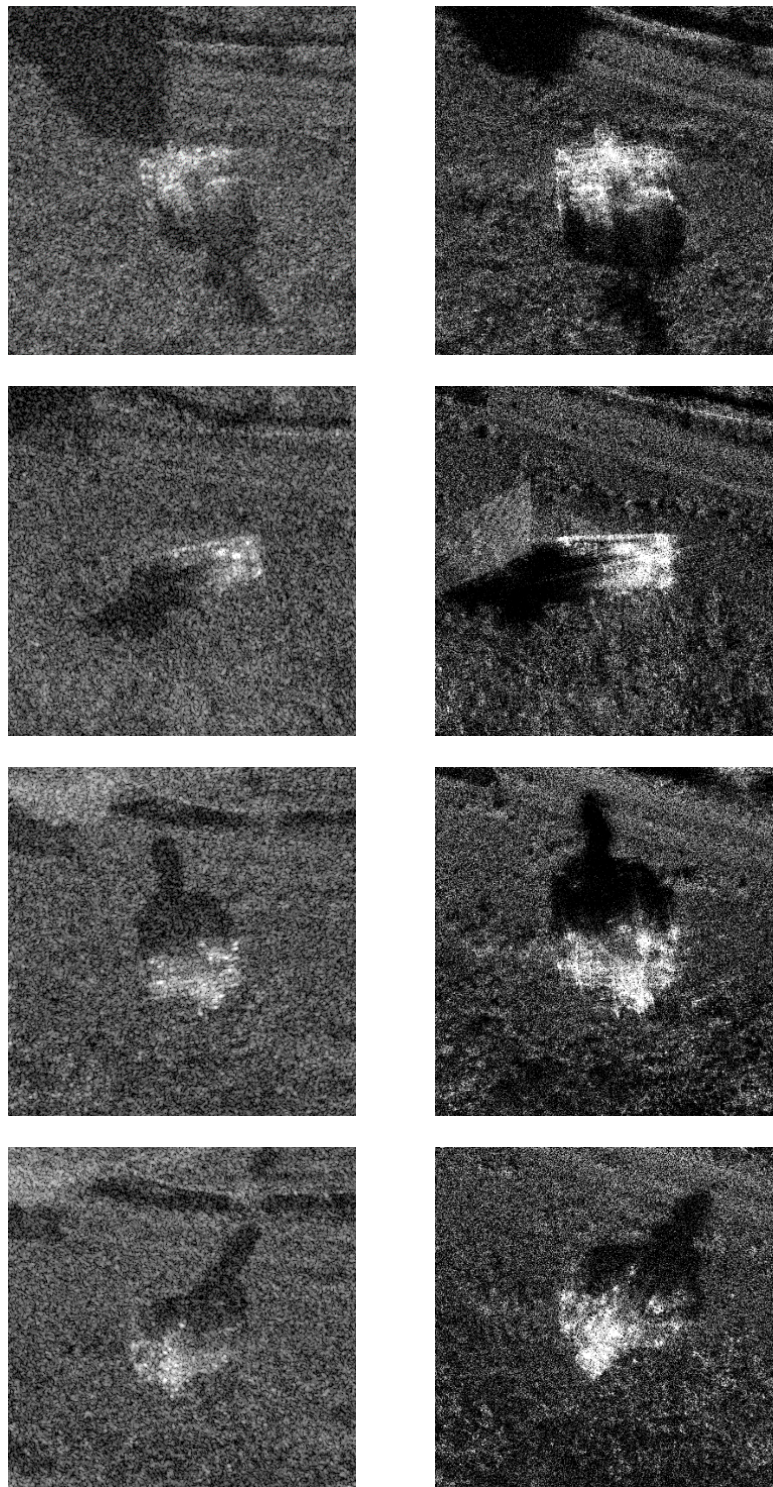


Figure 3: Images of target B; left and right column show PAMIR-Ka and MIRANDA-94 results, respectively

Figure 3 shows the resulting SAR image segments of target B with the same aspect angles as target A before. On the first images of both PAMIR-Ka and MIRANDA-94, a shadow appears that indicates a higher structure on top of the vehicle. This is caused by an antenna on top of the vehicle. The images in the second row give again a good impression of the width of the target. The shadow of the side view in the third row

gives very detailed information about the silhouette of the target. Due to the classification of this contribution, we are not allowed to show optical images of the targets for comparison.

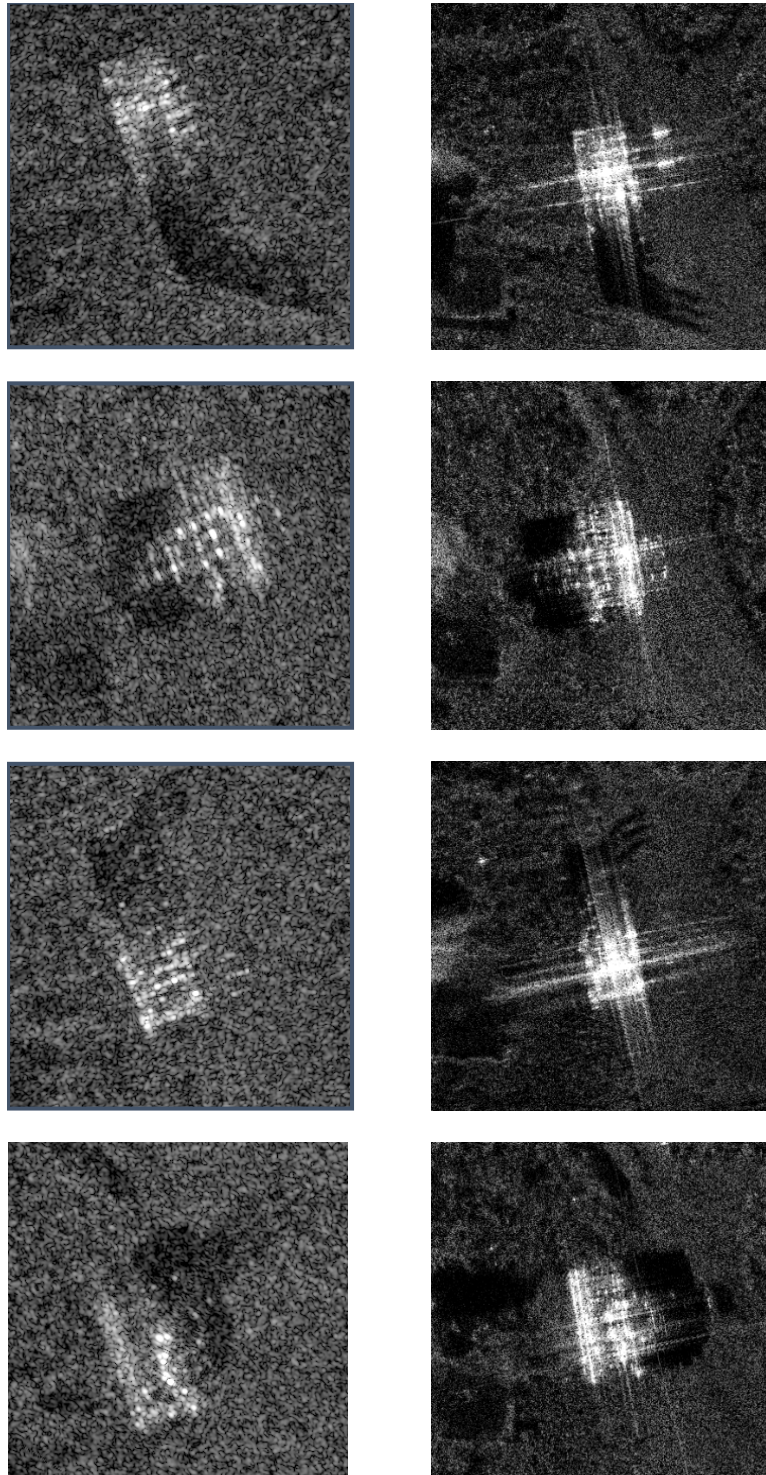


Figure 4: Images of target C; left and right column show PAMIR-Ka and MIRANDA-94 results, respectively

We collected the results of target C in Figure 4. In the SAR images of the first and third row, the three missiles can be clearly identified from the shadows. In addition, reflections from the foreparts of the missiles can be observed in the first image of MIRANDA-94 and the third image of PAMIR-Ka.

As can be seen, the images of both SAR systems provide similar information about the three targets. However, the images differ in some aspects. We observe a lower dynamic in the images of PAMIR-Ka than in those of MIRANDA-94. The shadows seem to be more noisy and the target reflections are weaker. Both can be explained by the already mentioned fact that the ground clutter reflection is stronger in W-band. Scene parts that seem to be specular in Ka-band might appear scattering for the higher frequencies. Another effect leads to a better visibility of the shadows in the images of MIRANDA-94. For a given cross range resolution the synthetic aperture length can be much shorter than for the PAMIR-Ka acquisitions, so that the edge of the shadow is sharper in the MIRANDA images. On the other hand, the images of MIRANDA-94 suffer from the very strong reflections of corner-like structures of the targets. Side lobes of these corner reflections superpose other parts of the target, consequently hindering the analyses of the target structure.

3.0 POLARIMETRIC SAR IMAGING

Since the MIRANDA-94 system has two receive channels with polarisation directions perpendicular to each other, this system collected V- and H-components throughout the campaign. Figure 5 shows the RGB composite of target A for the selected observation angles, where red belongs to the co-polarisation, green to the cross-polarisation, and blue is the difference between the co- and cross-polarised channel.

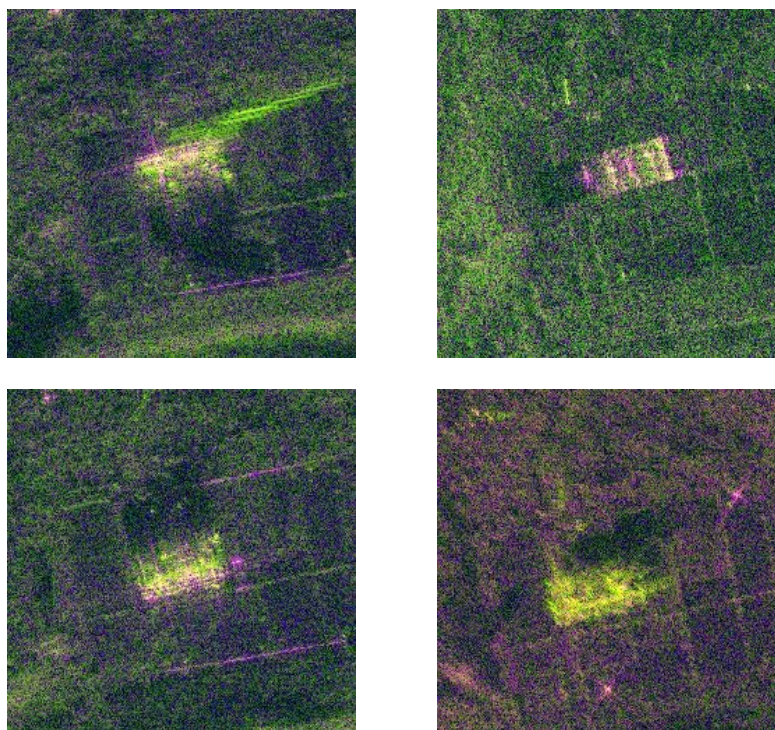


Figure 5: Polarimetric SAR images of target A acquired with MIRANDA-94 (red: co-polar channel; green: cross-polar channel, blue: difference between co- and cross-polarised channel)

The polarimetric representation makes the SAR images appear much more detailed and natural compared to the non-polarimetric ones. Man-made objects often stand out more clearly, which is particularly evident for the edges of the vehicle. It is not clear why the scenery around the target in the second image can be seen so

strongly in the cross-polarised channel (coloured green), while this is not obvious in the other images.

Polarimetric measurements support the thorough analysis of SAR images and increase the information content significantly. For the future, we plan to equip the MIRANDA-94 frontend with a second transmission channel to enable fully polarimetric measurements with the system.

4.0 MULTI-LOOK IMAGING

In this section, we use one measurement of the SET-250 trials to demonstrate the effect of multi-look processing. PAMIR-Ka is using standard gain horn antennas to transmit and receive the radar signals in the current development stage. This leads to an observation angle of each point in the scene that is much wider than the integration angle for the desired azimuth resolution. A part of this surplus is valuable to be robust with respect to drift variation of the aircraft. The remaining observation angle is used here for multi-look processing.

The data have been processed with a GPU based standard backprojection processor. Windowing of range frequency and azimuth is applied to achieve 10 cm resolution in both azimuth and ground range. The processed signal bandwidth is much smaller than the available signal bandwidth of the measurements. Thus, multiple looks can be generated in addition for independent frequency bands. Therefore, based on the total available band of the selected measurement of 4 GHz, we specified two sub-bands of 1.7 GHz each without overlap.

To realize the multiple looks in azimuth, five different observation angles on ground with an offset of 2° between adjacent looks were evaluated. This results in a slight overlap of adjacent angular looks according to a coherent integration angle of 2.7° for each single SAR image. Because of uncompensated motion errors, a misalignment was present between the different angular looks. This has been corrected using a co-registration algorithm according to Ref. [5].

4.1 Multi-look incoherent overlay

Figure 6 contains in the top part a single look SAR image of the scene that belongs to the optical GoogleEarth image already shown in Figure 1. The bottom part in Figure 6 shows the result of an incoherent overlay of the scene using the 10 looks from both observation angle and frequency. Due to this multi-look processing, the image has reduced speckle and the man-made objects appear more complete than in the standard single look SAR image.

The technical report [6] of the NATO SET-250 will contain a broad discussion of the advantages and the theoretical background related to the incoherent combination of SAR images that are acquired with different illumination directions.

4.2 A peculiar man-made object

In the area of the orange rectangle in the bottom SAR image of Figure 6, an object with strong reflectivity appeared in some of the reconstructed looks, while other looks did not show this object at all. Some analyses showed that there is an object with a reflectivity that strongly depends on the illumination direction and the radar frequency. We modified the processing parameters so that we got three looks over frequency instead of the aforementioned two looks and reconstructed the SAR images of the marked scene part. Table 1 shows some looks of the marked area with three different illumination directions and three different centre frequencies. As can be seen, there is a rectangular object in the middle of this scene part with a strong reflectivity for 30° at centre frequency. If the illumination direction or the range frequency deviate a little bit,

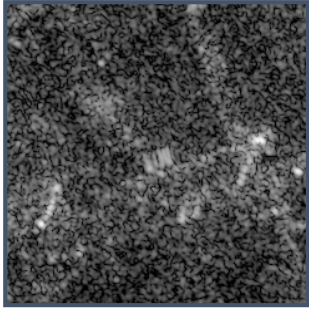
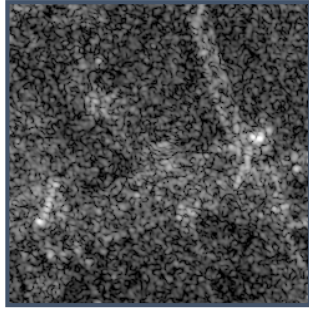
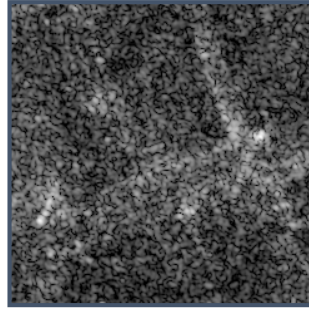
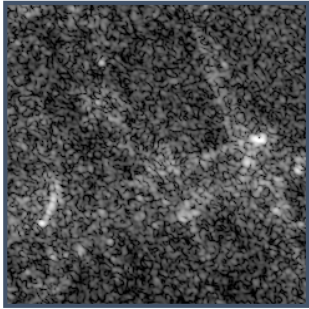
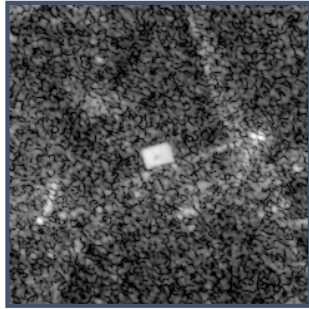
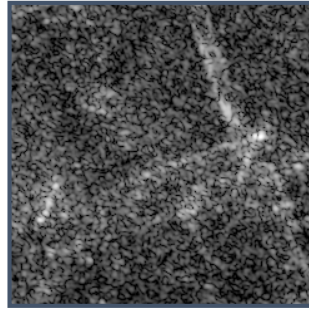
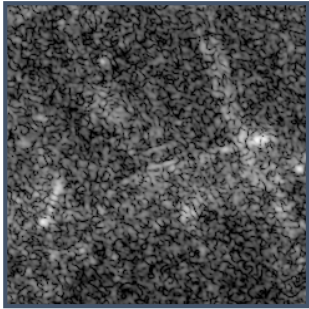
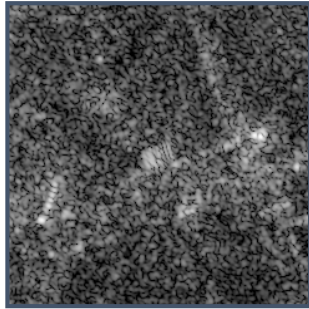
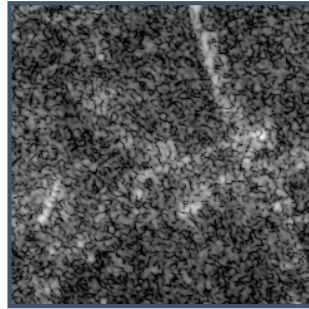
the reflectivity decreases considerably.



Figure 6: Comparison of a single look (top) and a multi-look SAR image (bottom). The rectangular mark is referenced in Section 5

It has been shown that a small change of illumination or processing parameters decides about the appearance of this object. An inquiry about this object revealed that there is a ventilation shaft at this point, which is probably covered with a grille. The selective reflectivity behaviour with respect to the illumination direction and the frequency should therefore come as no surprise.

Table 1: Images (different looks) of the man-made object, which probably represents a regular structure

	32°	30°	28°
+860 MHz			
centre frequency			
-860 MHz			

After this observation, we raised the question whether this object can be identified in the SAR images reconstructed from other acquisitions. Figure 7 shows SAR images of the marked region that we evaluated from SAR data of acquisitions with six different illumination directions. These images were processed with a range frequency window centred at the hardware centre frequency of PAMIR-Ka and a mean illumination angle that has been determined as an optimum for each acquisition before the backprojection. As can be seen, the rectangular object appears doubtless in just one SAR image (last SAR image in clockwise direction), which is just that one from the discussion before. As the second image in clockwise direction at least shows some structure at the position of the object, we evaluated looks by varying the processing frequency and the illumination direction for this acquisition. Figure 8 shows results of two looks. The left sub-image contains the SAR image reconstructed with the standard processing parameters and the right sub-image shows the result with an 860 MHz higher processing centre frequency and a 2° lower illumination direction window. The rectangular object is clearly visible in the second image.

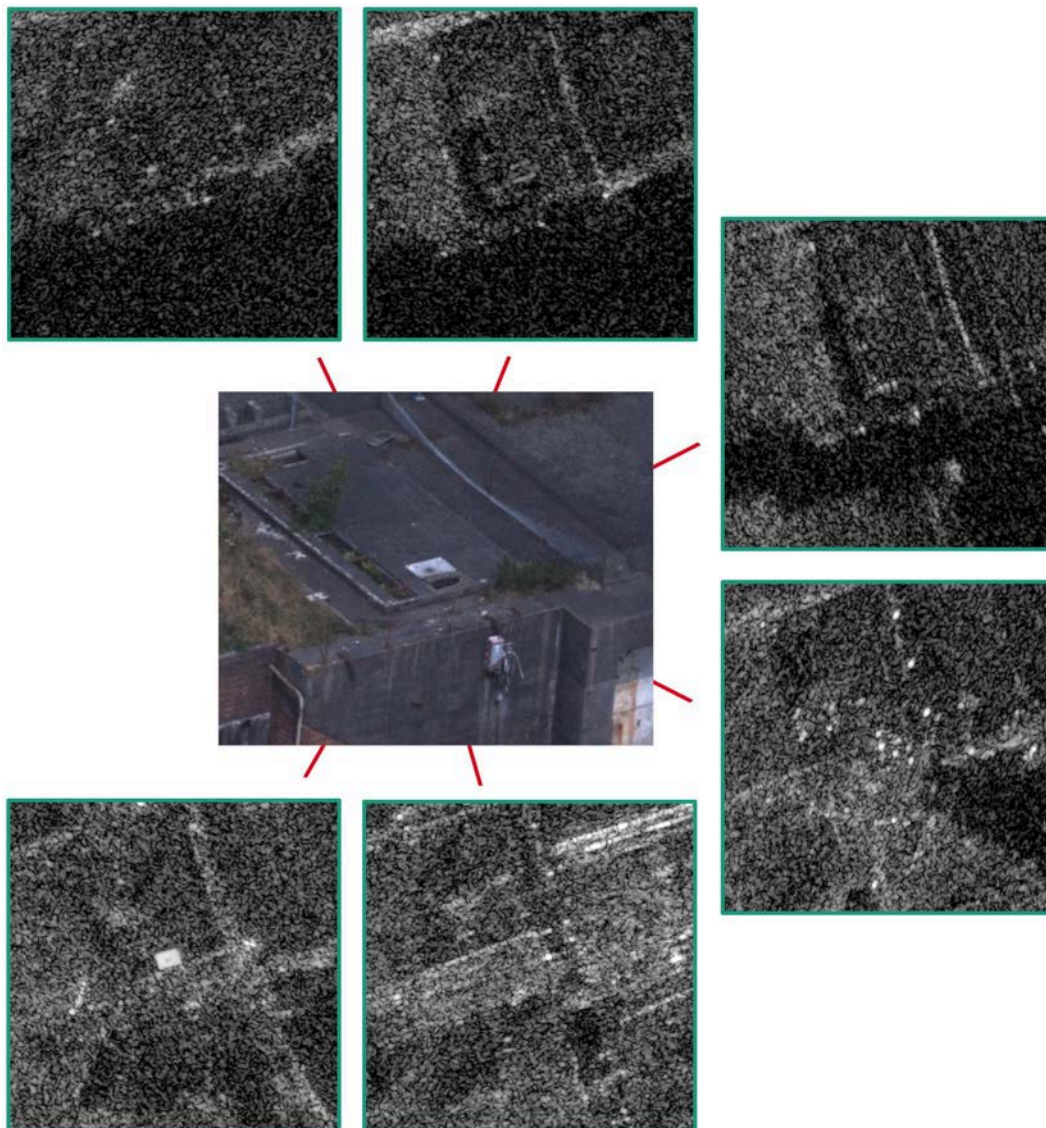


Figure 7: Optical image of the rectangular object (structured plate or grid) and six SAR images acquired from different directions around the optical image

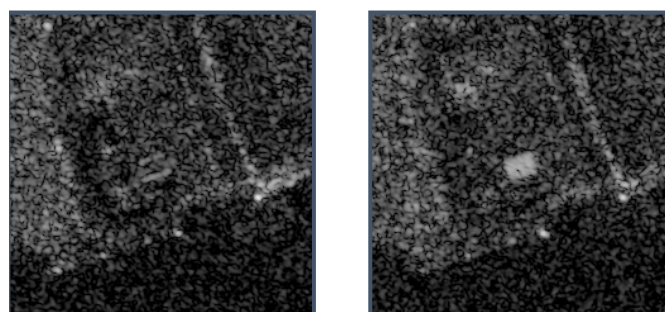


Figure 8: SAR images of two looks from the second acquisition in clockwise direction: left image processed with centre frequency 35 GHz and 202° illumination direction and right image processed with centre frequency 35.86 GHz and 200° illumination direction

5.0 CONCLUSION

In this contribution, we presented results of SAR acquisitions that we performed during the joint radar trials of the NATO SET-250 in England with our SAR systems PAMIR-Ka and MIRANDA-94. After a brief introduction, we focussed on three military targets that were illuminated from different directions. As can be seen, different target features are visible from the different observation directions and a collection of all images offers much more information than any single SAR image. Both radar bands, Ka- and W-band, seem to have individual advantages with respect to image contrast, sharpness of shadow, sensitivity/robustness with respect to corner-like structures, and others. However, it is difficult to derive general rules here, as the two systems differ in many more aspects than just the frequency band of operation.

Using the polarimetric feature of the MIRANDA-94, we generated colour-coded half-polarimetric images of a selected target and discussed some advantages of this system capability.

Based on acquisitions of the PAMIR-Ka system, we performed multi-look processing in both range frequency and observation direction. In this context, we demonstrated two promising approaches: First, an overlay of multiple looks seems to result in a SAR image that is ‘more complete’ for a human viewer and second, a combined analysis of multiple looks might have potential for target recognition as difference (or similarity) between looks can be used as an additional recognition aspect.

6.0 REFERENCES

- [1] Martorella, M., Greig, D., Caris, M., Trampuz, C., and Zihlmann, A. (2021). Multi-dimensional radar data collection trial for NATO SET 250. SET-273 Research Specialists’ Meeting on Multidimensional Radar Imaging for Automatic Target Recognition, Marseille, 25 – 26 Oct 2021.
- [2] Walterscheid, I., Berens, P., Caris, M., Sieger, S., Saalman, O., Janssen, D. et al. (2020). First results of a joint measurement campaign with PAMIR-Ka and MIRANDA-94. 2020 IEEE Radar Conference (RadarConf20), pp. 1-6.
- [3] Caris, M., Stanko, S., Palm, S., Sommer, R., and Pohl, N. (2015). Synthetic aperture radar at millimeter wavelength for UAV surveillance application. Proc. RTSI 2015, Torino (I), pp. 349-352.
- [4] El-Arnauti, G., Saalman, O., and Brenner, A.R. (2018). Advanced system concept and experimental results of the ultra-high resolution airborne SAR demonstrator PAMIR-Ka. EUSAR 2018; 12th European Conference on Synthetic Aperture Radar, pp. 1-5.
- [5] Ribalta, A. (2020). Extending the FOLKI-PIV algorithm for the coherent coregistration of SAR images. IGARSS 2020, pp. 2001-2004.
- [6] NATO STO. Multi-dimensional radar imaging. Technical Report STO-TR-SET-250, NATO STO, Neuilly-sur-Seine, France (in preparation).

